Science Bulletin 69 (2024) 2420–2429

Contents lists available at ScienceDirect

Science Bulletin

journal homepage: www.elsevier.com/locate/scib

Article

Reconciling East Asia's mid-Holocene temperature discrepancy through vegetation-climate feedback

Jie Chen [a], Qiong Zhang [b,*], Zhengyao Lu [c], Yanwu Duan [d], Xianyong Cao [d], Jianping Huang [e], Fahu Chen [a,d]

[a] Key Laboratory of Western China's Environmental Systems (Ministry of Education), College of Earth and Environmental Sciences, Lanzhou University, Lanzhou 730000, China
[b] Department of Physical Geography and Bolin Centre for Climate Research, Stockholm University, Stockholm 10691, Sweden
[c] Department of Physical Geography and Ecosystem Science, Lund University, Lund 22100, Sweden
[d] Group of Alpine Paleoecology and Human Adaptation (ALPHA), State Key Laboratory of Tibetan Plateau Earth System, Environment and Resources (TPESER), Institute of Tibetan Plateau Research (ITPCAS), Chinese Academy of Sciences (CAS), Beijing 100101, China
[e] Collaborative Innovation Center for Western Ecological Safety, Lanzhou University, Lanzhou 730000, China

ARTICLE INFO

Article history:
Received 11 May 2023
Received in revised form 28 February 2024
Accepted 7 March 2024
Available online 7 April 2024

Keywords:
Holocene temperature conundrum
Holocene Thermal Maximum
Vegetation-climate feedback
East Asia
Paleoclimate simulations

ABSTRACT

The term "Holocene temperature conundrum" refers to the inconsistencies between proxy-based reconstructions and transient model simulations, and it challenges our understanding of global temperature evolution during the Holocene. Climate reconstructions indicate a cooling trend following the Holocene Thermal Maximum, while model simulations indicate a consistent warming trend due to ice-sheet retreat and rising greenhouse gas concentrations. Various factors, such as seasonal biases and overlooked feedback processes, have been proposed as potential causes for this discrepancy. In this study, we examined the impact of vegetation-climate feedback on the temperature anomaly patterns in East Asia during the mid-Holocene (~6 ka). By utilizing the fully coupled Earth system model EC-Earth and performing simulations with and without coupled dynamic vegetation, our objective was to isolate the influence of vegetation changes on regional temperature patterns. Our findings reveal that vegetation-climate feedback contributed to warming across most of East Asia, resulting in spatially diverse temperature changes during the mid-Holocene and significantly improved model-data agreement. These results highlight the crucial role of vegetation-climate feedback in addressing the Holocene temperature conundrum and emphasize its importance for simulating accurate climate scenarios.

1. Introduction

The "Holocene temperature conundrum" refers to the discrepancy between proxy-based reconstructions and transient model simulations of global annual mean surface air temperature (SAT), and it challenges our understanding of temperature evolution during the Holocene. Climate reconstructions suggest a cooling trend following the Holocene Thermal Maximum (HTM) (~10–6 ka) towards the pre-industrial period (PI) [1,2], while transient model simulations indicate a consistent global warming trend throughout the Holocene in response to ice-sheet retreat and rising greenhouse gas (GHG) concentrations [3]. This inconsistency has persisted despite recent efforts to integrate global reconstruction data and model temperatures using paleoclimate data assimilation [4–6].

One potential explanation for this conundrum is the occurrence of seasonal biases in reconstructions [3,7,8]. However, recent seasonal temperature records from the Northern Hemisphere do not support this explanation, as they show a similar trend to annual mean records [9–11]. Deficiencies in model simulations, such as the underestimation of climate sensitivity (e.g., Arctic amplification [12,13] and sea-ice loss [14,15]), and overlooking several feedback processes (e.g., dust feedback [16] and vegetation feedback [17,18]), could also influence global temperature changes. In particular, Thompson et al. [18] highlighted the importance of vegetation changes in resolving this conundrum. Their model simulations demonstrate systematically increased vegetation cover in the African Sahara, and in northern middle and high latitudes during the early and middle Holocene, in a high-end scenario as indicated by pollen records; their simulations indicate a ~0.4 ℃ warming during the mid-Holocene, mainly via enhanced net surface radiative flux [18], although their study may overestimate the influence of Northern Hemisphere

* Corresponding author.
E-mail address: qiong.zhang@natgeo.su.se (Q. Zhang).

https://doi.org/10.1016/j.scib.2024.04.012
2095-9273/

vegetation changes by prescribing the possible largest vegetation increase in this region.

Considering the complex spatio-temporal structure of the HTM in both reconstructions and climate simulations [19–23] (for instance, the model-data discrepancy is more prominent at low and middle latitudes [8,24]), it is essential to study the HTM from a regional perspective. East Asia has an abundance of temperature reconstructions and is thus an ideal region for addressing the conundrum [25]. Pollen records from East Asia reveal a heterogeneous pattern of Holocene vegetation changes [26], making the influence of the vegetation-climate feedback on the HTM uncertain. Thus, understanding the dynamic response of vegetation to climate forcing and the resulting feedback is crucial for accurate future climate predictions.

In this study, we used the fully coupled Earth system model EC-Earth (version 3.3) to investigate the impact of vegetation changes on the temperature variations in East Asia during the mid-Holocene. By conducting simulations with and without coupled dynamic vegetation, we aimed to distinguish the influence of vegetation changes on temperature patterns in this region. Our simulations accurately reproduced global vegetation changes in the mid-Holocene, such as large-scale vegetation expansion in the Sahara [27] and northern high latitudes [28], a decrease in vegetation in the Amazon [29] (Fig. S1 online), and local vegetation changes in East Asia (see Results). Our results suggest that a vegetation-climate feedback mechanism could have warmed most parts of East Asia and led to a spatially diverse pattern of temperature change during the mid-Holocene, significantly improving the level of model-data agreement in this region.

2. Materials and methods

2.1. Earth system model simulations

We conducted simulations using the fully coupled Earth system model EC-Earth (version 3.3), the Coupled Model Intercomparison Project Phase 6 (CMIP6) version of the European Consortium Earth System Model [30]. EC-Earth includes the Integrated Forecast System (IFS) with 62 vertical levels, the land model H-TESSEL [31], the Nucleus for European Modeling of the Ocean (NEMO3.6) with 75 vertical levels [32], the Louvain-la-Neuve sea ice model (LIM3) [33], and the second-generation dynamic vegetation-ecosystem model (LPJ-GUESS) [34] (see Supplementary Note 1 and Table S1 online). EC-Earth reliably reproduces major vegetation and temperature features in East Asia (see Supplementary Note 2 and Fig. S2 online).

We conducted four simulations: Two with coupled dynamic vegetation (PI_veg, MH_veg) and two without (PI_orb, MH_orb), all under pre-industrial and mid-Holocene orbital and GHG conditions, as per the Paleoclimate Model Intercomparison Project Phase 4 (PMIP4) protocol (Table S2 online). We initialized the simulations using the end of the PI spin-up phase, followed by another 200-year spin-up period to reach a new equilibrium. We then analyzed the subsequent 200 years of data (see Supplementary Note 1 online).

There is a substantial difference in orbital forcing and minor variations in GHG concentrations between the PI and mid-Holocene simulations (Table S2 online). Thus, the differences we identified between MH_orb and PI_orb predominantly reflect changes in climate resulting from differences in orbital forcing. The influence of GHG concentrations (ΔOrb + ΔGHG = MH_orb − PI_orb), although present, is relatively minor in this context. Furthermore, the climate changes encompassing differences in orbital forcing, GHG concentrations, and vegetation-climate feedback are represented by the differences between MH_veg and PI_veg (ΔOrb + ΔGHG + ΔVeg = MH_veg − PI_veg). This approach allows us to capture the impact of these combined factors on climate. To isolate the specific component attributed to vegetation changes and vegetation-climate feedback, we calculated the difference between these two sets of simulations (ΔVeg = (MH_veg − PI_veg) − (MH_orb − PI_orb)). This calculation method effectively distinguishes the vegetation-climate feedback from the overall climate changes observed between the mid-Holocene and PI.

2.2. Offline LPJ-GUESS simulations

To determine the impact of climate changes on vegetation changes in East Asia during the mid-Holocene, we performed five simulations using the offline dynamic vegetation model LPJ-GUESS. The model was driven by atmospheric variables from the PI_veg simulation. We conducted two groups of four sensitivity experiments to isolate the effects of precipitation and temperature changes (Table S3 online), systematically increasing summer precipitation by 40% and adjusting the temperature values based on the PI simulation (see Supplementary Note 3 and Figs. S3 and S4 online).

2.3. PMIP4 simulations

We compiled 13 PMIP4 simulations with prescribed vegetation to compare annual SAT differences between the mid-Holocene and PI (Table S4 online). All data were re-gridded to T159 resolution ($\sim$1.125°) using bilinear interpolation, following the resolution of EC-Earth output, to facilitate comparison.

2.4. Model-data comparison

We compared the reconstructed temperatures from the Temperature 12k database (Temp 12k v1.0.0) [4] and records of pollen assemblages and glycerol dialkyl glycerol tetraethers (GDGTs) (Supplementary Data 2 online) with the simulated SAT differences (see Supplementary Note 4 online). We also conducted a preliminary model-data comparison between vegetation types simulated by our model with biome records based on pollen and plant macrofossil data from BIOME6000 for the PI and mid-Holocene periods [35]. To compare the vegetation categories, we followed the methods in Prentice et al. [36] (see Table S5 online), considering a match if one or more grid cells around a biome reconstruction within 1.125° radius showed the same vegetation types.

Overall, we adopted a multi-faceted approach to analyze the impact of vegetation changes on climate during the mid-Holocene in East Asia. By utilizing Earth system model simulations, offline LPJ-GUESS simulations, PMIP4 simulations, and model-data comparisons, we aimed to provide a comprehensive understanding of the vegetation-climate feedback and its implications for future climate predictions.

3. Results

3.1. Temperature changes in East Asia

The multi-model ensemble of 13 models from PMIP4 shows an overall cooling in East Asia during the mid-Holocene compared with PI (Fig. 1a). All these simulations used prescribed vegetation, as in PI. Our simulations with prescribed vegetation show similar cooling results but scattered warming, especially in northern East Asia (Fig. 1a, b). These inconsistencies between the PMIP4 ensemble mean results and our simulations persist among individual PMIP4 model results (Fig. S5 online), indicating significant uncertainties in simulating East Asia climate. Proxy reconstructions in

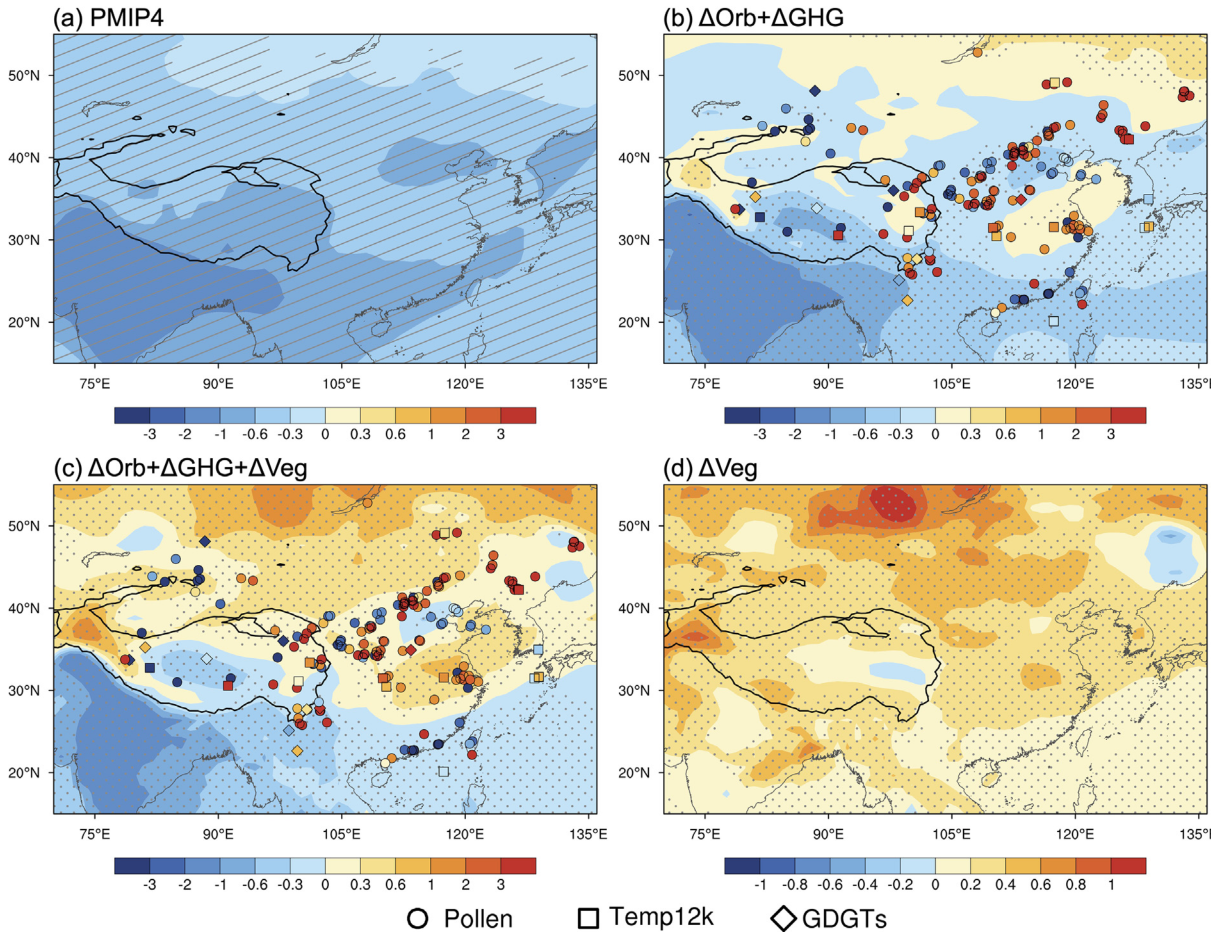

Fig. 1. Comparison of annual mean SAT (unit: ℃) changes in the mid-Holocene relative to PI between simulations and reconstructions. (a) Ensemble annual mean SAT changes for 13 PMIP4 model simulations. Annual mean SAT changes due to (b) orbital forcing and GHG concentrations (ΔOrb + ΔGHG); (c) the combination of orbital forcing, GHG concentrations, and vegetation-climate feedback (ΔOrb + ΔGHG + ΔVeg); and (d) vegetation-climate feedback (ΔVeg). The oblique lines in (a) indicate that the SAT changes are consistent (in phase) across more than 10 models. The dots represent values exceeding the 95% confidence level, calculated using a Student's *t*-test on the 200-year simulation following the spin-up period. Areas above 3,000 m (above sea level) are enclosed by heavy black lines. A detailed description of the reconstruction data can be found in Supplementary Note 4 and Supplementary Data 2 (online).

East Asia correspond more closely with our simulation results, suggesting a warmer mid-Holocene climate, although discrepancies remain between proxy records and our simulations and PMIP4 simulations: for example, in North China and the eastern and northern Tibetan Plateau (TP).

When including dynamic vegetation, our model simulated spatially heterogeneous temperature changes, with large-scale warming in northern East Asia comprising Central, North, and Northwest China, Mongolia and Siberia, and cooling in the southern region comprising the southern TP, South China, and South China Sea (Fig. 1c). Vegetation-climate feedback induces warming in North and Northwest China and intensifies the warming in Northeast China, Mongolia, and Siberia (Fig. 1c, d). This warming effect, due to vegetation changes, occurs year-round and offsets cooling in winter and spring while amplifying warming in summer and autumn (Fig. S6 online), as a result of orbital forcing and GHG concentrations [3,8].

Comparisons between proxy reconstructions and simulated temperature changes reveal that simulations with dynamic vegetation are in better agreement with reconstructions in East Asia. Model-data consistency increased from ~48% with prescribed vegetation, to ~61% with significant improvements in Central China, Northeast China, and the TP (Table S6 and Fig. S7 online). Our simulations capture regional cooling in North China, which is consistent with nearby reconstructions (Fig. 1c). While our study only includes a few quantitative proxies from the Mongolia Plateau, most published qualitative proxy data suggest a warming climate in the mid-Holocene compared with PI [37,38]. We propose that vegetation-climate feedback significantly contributed to the spatial heterogeneity of temperature changes in East Asia during the mid-Holocene.

3.2. Vegetation changes in East Asia

Our model simulated an expansion of needleleaf trees in semi-arid regions during the mid-Holocene compared with PI (Fig. 2), consistent with other studies [28,39]. The simulated vegetation distribution corresponds well with the results of BIOME6000, with agreement rates of ~71% for the PI and ~67% for the mid-Holocene (see Materials and Methods). However, substantial disagreement persists in Northeast China; nevertheless, the model results indicate that some areas of evergreen needleleaf trees in Northeast China were replaced by mixed forest (a mixture of evergreen needleleaf trees and deciduous broadleaf trees) during the mid-Holocene, which is consistent with pollen records that show an increase in broadleaf deciduous forest cover and a decrease in coniferous forest cover at this time [26,40].

Simulated forest cover significantly increased in North China and southern Siberia during the mid-Holocene, matching the expansion of forest in these areas (Figs. 2 and 3a). Decreased forest cover is observed in Northeast, South and Central China. These simulated forest cover changes are largely consistent with biome

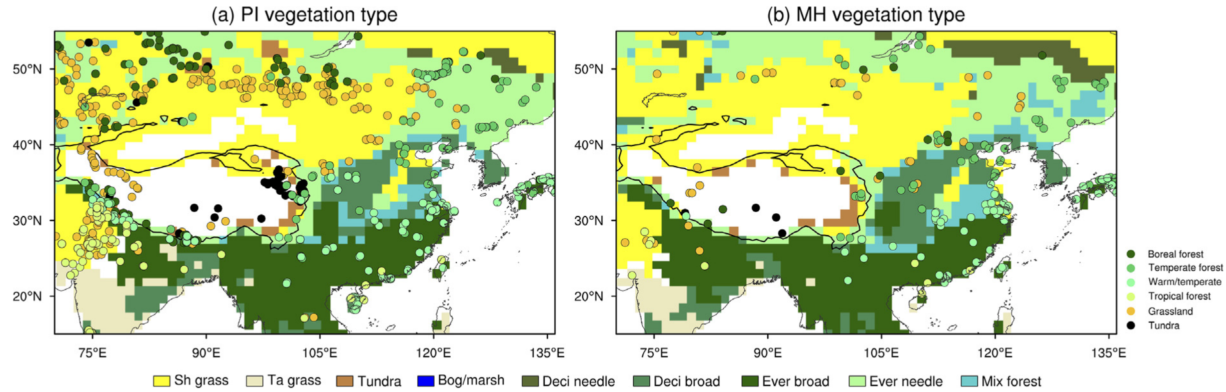

Fig. 2. Distribution of the dominant vegetation types in East Asia. Dominant vegetation types simulated by EC-Earth (color shading) and revealed by reconstructed biomes (dots) in (a) PI and (b) mid-Holocene (MH). Bare soil (white shading) is shown where the vegetation cover is less than 15%. The reconstructed biomes in the mid-Holocene are derived from the BIOME6000 dataset [35].

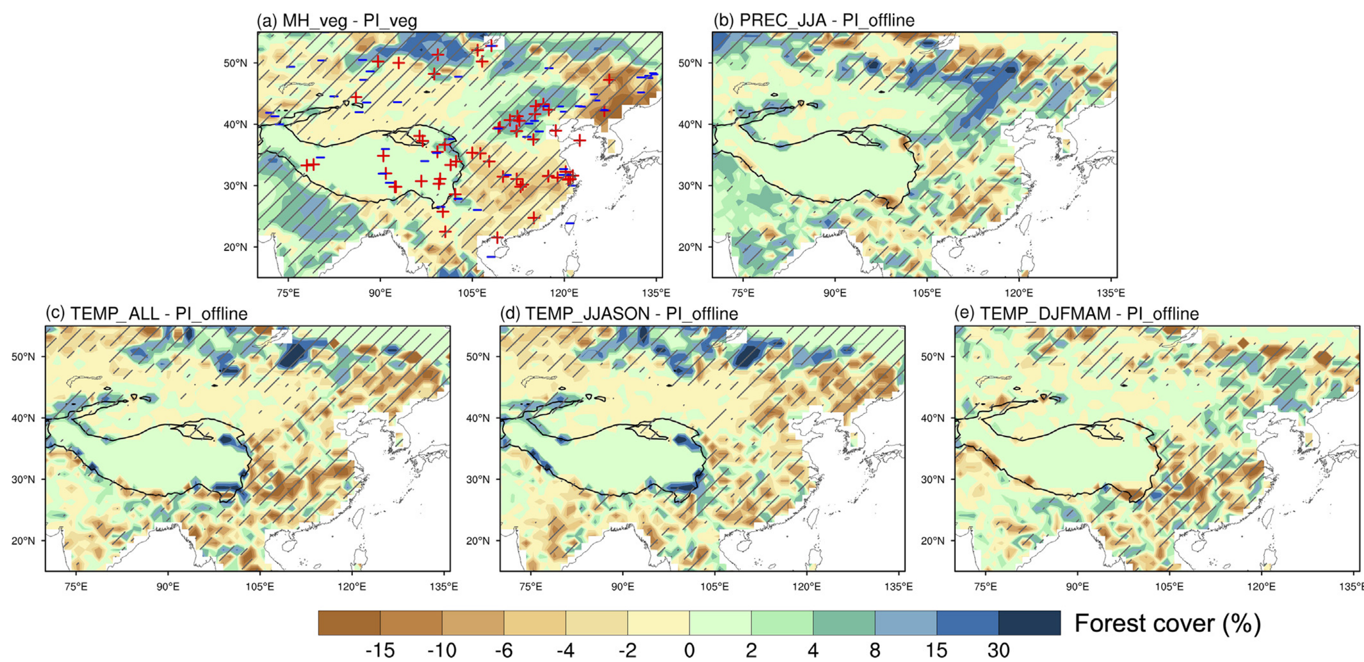

Fig. 3. Simulated changes in forest cover. Simulated annual mean forest cover changes (color shading) for the (a) mid-Holocene using EC-Earth and (b–e) various sensitivity experiments using the offline dynamic vegetation model LPJ-GUESS (see Table S3 online). Blue minus (−) symbols indicate a decrease and red plus (+) symbols indicate an increase in forest cover, as shown by pollen records [26,46,47]. The oblique lines represent values that exceed the 95% confidence level based on a Student's *t*-test.

reconstructions, except for South and Central China, which show the opposite results (Fig. 3a). The discrepancies potentially result from human activities, as the biome reconstructions incorporate signals of human activity [41–44], whereas the simulated vegetation does not. In contrast, the changes in areas with low vegetation cover are much more subtle than in forested regions (Fig. S8a online). Increased low vegetation cover is found in the eastern part of the arid region, dominated by grassland, and southern TP, corresponding well with the biome reconstructions [45,46]. In forest-dominated areas, changes in the cover of low vegetation generally oppose the changes in forest cover (Fig. 3a and Fig. S8a online).

3.3. Factors driving the simulated vegetation changes

To better understand the causes of the vegetation changes in East Asia, we performed four sensitivity experiments using the offline dynamic vegetation model LPJ-GUESS, to investigate the influence of temperature and precipitation on these changes (see Materials and Methods). The results indicate that forest cover changes in semi-arid regions during the mid-Holocene were mainly driven by changes in summer precipitation (Fig. 3a, b). As a result, grasses decreased and the dominant evergreen needleleaf trees expanded westward (Fig. S9 online). This suggests that enhanced monsoonal precipitation during the mid-Holocene, induced by orbital forcing [48,49], largely accounts for the vegetation changes in this region (Fig. 3b and Figs. S8b and S9b online), as also demonstrated by reconstructed results from previous studies [26,47,50,51].

Regarding the impact of temperature on vegetation, the combination of summer and autumn warming, and winter and spring cooling—which follows the pattern of solar insolation differences between the mid-Holocene and PI (Fig. S4 online)—mainly controlled the forest cover in South, Central, and Northeast China, and southern Siberia (Fig. 3c–e). Specifically, summer-autumn warming led to a distinct decrease in forest cover in South and Northeast China and an increase in southern Siberia, whereas winter-spring cooling resulted in decreased forest cover in Central

China (Fig. 3d, e). These findings align with tree-ring records, which suggests that tree growth in Central China and Northeast China is significantly influenced by winter-spring [52,53] and summer [54,55] temperatures, respectively. Furthermore, the replacement of evergreen needleleaf trees with mixed forest in Northeast China is attributed to temperature changes (Fig. S9 online). The underlying mechanisms can be interpreted as follows: Cool winter and spring temperatures cause a delayed start to the growing season for evergreen broadleaf trees in Central China [56]; while warm summer-autumn temperatures constrain the growth of needleleaf trees and favor the transition from evergreen needleleaf trees to deciduous broadleaf trees in Northeast China, and favor the growth of evergreen needleleaf trees in southern Siberia where temperatures are lower than in Northeast China (Fig. S10 online). Consequently, we conclude that temperature was the main factor controlling the vegetation changes in Central and Northeast China and southern Siberia during the mid-Holocene. Additionally, changes in low vegetation are less dependent on temperature changes, except for a significant increase in tundra on the southern TP (Fig. S9c–e online), indicating that the

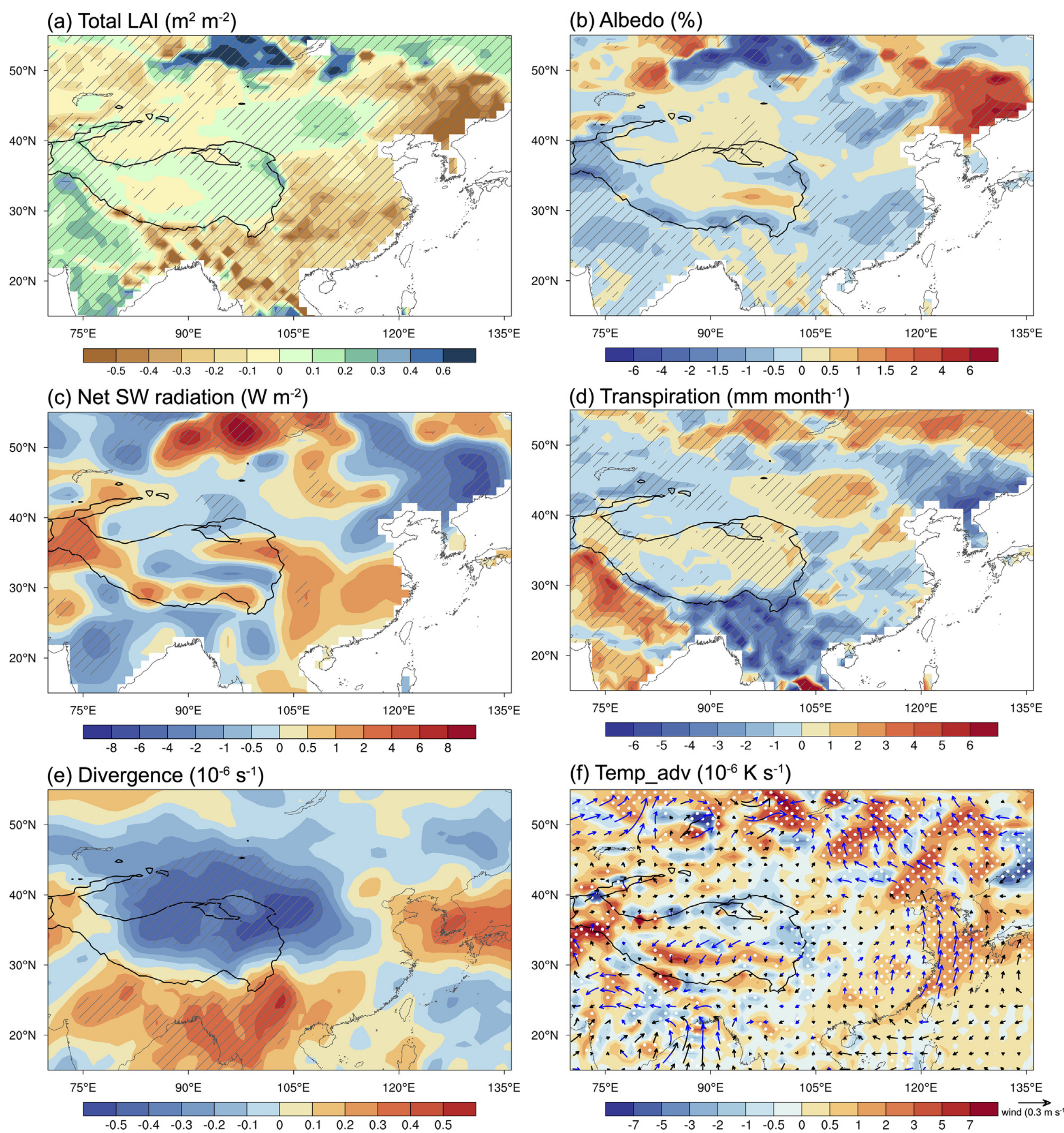

Fig. 4. Biophysical processes and atmospheric anomalies in response to vegetation changes in the mid-Holocene. (a) Annual mean total leaf area index (LAI) difference due to vegetation changes, (b) surface albedo, (c) net shortwave (SW) radiation, (d) transpiration, (e) 200 hPa divergence, and (f) surface temperature advection ($-V \cdot \nabla T$) and wind (10 m above ground) anomalies, due to vegetation-climate feedback (ΔVeg). The total LAI is defined following van den Hurk et al. [57] as $LAI_T = C_H \times LAI_H + C_L \times LAI_L$, where C_H and C_L represent forest and low vegetation cover, respectively; LAI_H and LAI_L represent the LAI of forest and low vegetation, respectively. The oblique lines and white dots represent values exceeding the 95% confidence level based on a Student's *t*-test. The blue vectors in (f) indicate that the wind speeds exceed the 95% confidence level.

increase in low vegetation during the mid-Holocene was also mainly driven by temperature changes.

3.4. Mechanisms of vegetation-climate feedback to temperature

In general, an increase in vegetation is accompanied by a decrease in surface albedo. Our simulated results reveal that surface albedo decreases in the semi-arid region, southern Siberia, and increases in Northeast China during the mid-Holocene, compared with the PI, which is consistent with this negative relationship (Fig. 4a, b). However, the reduced surface albedo in Central and South China indicates a positive relationship with vegetation changes in these areas. This result is also observed in other global model simulations [58,59] and in present-day satellite remote sensing results [60–62]. This is mainly attributed to the fact that bare soil has a lower albedo than the covered surface in Central and South China in the model (Fig. S11 online). The reduced vegetation, coupled with an increase in bare soil in Central and South China, contributes to the overall decrease in surface albedo. The increased brightly leafy canopy and decreased darker gaps caused by forest greening also potentially lead to an increased albedo [61]. Consequently, these surface albedo increases (decreases) result in weakened (enhanced) surface net shortwave radiation (net SW) (Fig. 4c), contributing to warming in the semi-arid regions, southern Siberia, Central and South China, and cooling in Northeast China.

In addition to the albedo effect, evapotranspiration (ET) plays a more significant role in modulating temperature changes in East Asia. Several studies suggest that the greening-induced evaporative cooling could offset the radiative warming caused by the albedo effect in eastern China and the TP at the present day [59,63,64]. Our results reveal that transpiration changes roughly follow vegetation changes. Enhanced evaporative cooling may offset radiative warming in the semi-arid region and eastern TP, leading to net cooling. Weakened evaporative cooling strengthens the warming caused by the albedo effect in Central and South China and limits the radiative cooling in Northeast China. Considering that the increase of forest in southern Siberia has a warming effect [65], we suggest that the positive net SW anomalies overcome the evaporative cooling in southern Siberia (Fig. 4c, d), resulting in net warming. Thus, local vegetation changes could cause net warming in South and Central China and southern Siberia.

Besides the vegetation-induced albedo and ET effect, the atmospheric circulation anomalies may also contribute to warming in East Asia. Convergence anomalies resulting from the vegetation-climate feedback occur over the TP, Northwest and Northeast China in the upper troposphere, indicating anomalous descending motion accompanied by anomalous adiabatic warming in these areas [48,66] (Fig. 4e). Moreover, the equivalent barotropic structure of positive geopotential height anomalies, with positive centers over northwest China–TP and northeast China–northern North Pacific in East Asia (Fig. S12 online), favors the anomalous convergence and descending atmospheric motion in these regions [67]. These findings suggest that the anomalous descending atmospheric motion resulting from the large-scale atmospheric circulation anomalies contributes to local warming in these areas. Additionally, temperature advection anomalies may contribute to warming in East Asia. Southerly wind anomalies in response to the anomalous high-pressure system over Northeast China could bring anomalous warmer air from the North Pacific to Northeast China and southern Siberia, promoting warming in these regions (Fig. 4f).

It is important to note that these geopotential height anomalies in East Asia appear to be a part of a global teleconnection wave train (Fig. S12 online). Large-scale vegetation changes, such as the expansion of vegetation in the Sahara and in northern high latitudes, have the potential to induce this teleconnection wave train [13,68,69]. However, the underlying mechanisms behind this phenomenon require further study.

In summary, local albedo and ET changes, along with atmospheric circulation anomalies resulting from vegetation changes, warmed most of the regions of East Asia during the mid-Holocene. This warming overcame the cooling induced by orbital forcing and GHG concentrations in northern East Asia and created spatially heterogeneous temperature changes during the mid-Holocene.

4. Discussion

4.1. Global temperature changes

From a global perspective, PMIP4 and our simulations with prescribed vegetation show global mean cooling of −0.3 ℃ and −0.1 ℃ during the mid-Holocene compared with PI, respectively (Fig. S13a, c online). Notably, these global temperature changes are the opposite to the reconstructed temperature changes, which suggests a global warming of ∼0.5 ℃ (Fig. S13e online). A key aspect of our research involves the coupling of a dynamic vegetation module. Our simulated results reveal a critical shift: The warming effect triggered by vegetation changes effectively offset the cooling impact attributed to orbital forcing and GHG concentrations. Consequently, this leads to a global mean warming of ∼0.1 ℃ during the mid-Holocene (Fig. S13d online). Although this warming is less pronounced than that in the simulations with a high-end scenario of vegetation expansion [18] and compared with proxy reconstructions [4], these results underscore the significant role of vegetation-climate feedback in improving global model-data agreement (Fig. S13b, d, and e online). Furthermore, our simulations successfully reproduced the warming pattern observed in reconstructions in northern middle and high latitudes (Fig. S13f online). In particular, the most significant improvement of the model-data agreement occurs in northern middle latitudes, and this finding is superior to the results presented in Thompson et al. [18] (Fig. S13f online). These results collectively highlight the importance of incorporating vegetation-climate feedback in climate models to achieve a more accurate representation of global temperature changes during the mid-Holocene.

4.2. Trend of temperature changes in East Asia after the HTM

Both climate reconstructions and our simulations reveal a spatially heterogenous pattern of temperature changes in East Asia during the mid-Holocene compared with PI. These changes feature a general cooling trend in northern East Asia and a warming trend in the south from the middle to late Holocene (Fig. 1c). However, model-data discrepancies exist in Southwest and Northwest China. Proxy data for Southwest China shows a positive annual temperature difference between the mid-Holocene and PI, which is the opposite to our simulations. Most proxies reveal a warming trend from the middle to late Holocene [70,71], and this discrepancy may partly result from the low temporal resolution of proxy records. It is worth noting that the absence of volcanic and solar influences, as specified in the PMIP4 protocol [21,72], may contribute to model-data discrepancies in temperature reconstructions for East Asia. Internal model biases may also contribute to these discrepancies.

Regarding the discrepancy in Northwest China, our simulated results show that vegetation-climate feedback overcame the warming trend induced by GHG concentrations [73]. This positive effect was also suggested by another study [18]. Since the changes in GHG concentrations between the mid-Holocene and PI are minimal (Table S2 online), we infer that the high model sensitivity to vegetation changes may cause the discrepancy. Overall, vegetation-climate feedback plays a crucial role in improving the model-data agreement and largely reconciles the Holocene temperature conundrum in East Asia. Given the significant influence of vegetation-climate feedback on modulating temperature changes, this vegetation-climate feedback may contribute to reducing the uncertainties in future temperature predictions.

4.3. Potential biases in the simulations

Our simulations show that vegetation changes respond well to the climatic differences between the mid-Holocene and PI (Fig. 3), but discrepancies between proxies and simulations persist in South and Central China. Previous studies proposed that human activities were a significant cause of forest cover decline in eastern China during the late Holocene, especially in South and Central China [41–44,74]. Our model simulations (both coupled EC-Earth and offline LPJ-GUESS) only account for the vegetation variations under different climate conditions, suggesting that this model-data discrepancy may result from human activities. We argue that human activities could be the main driver of the decrease in the forest cover in South and Central China and may also exacerbate the decrease in semi-arid regions, hence offset the forest cover increases in Northeast China during the late Holocene. Consequently, our simulation results may not fully represent the anthropogenic vegetation and climate change, leading to potential model biases.

Our model with dynamic vegetation is designed to simulate vegetation changes in East Asia in response to climate change. By accurately reproducing past vegetation changes, the model can help us better understand how vegetation responds to different climate conditions and how it may continue to change in the future. Our results regarding the impact of precipitation and temperature changes on the summer vegetation changes offer useful insights into the implications of pollen records in different areas.

The discrepancy between simulated vegetation changes and those indicated by pollen records suggests that the actual climatic impact of these vegetation changes may differ from our simulation results. Notably, previous studies indicate that the transition from forest to cropland in the PI led to surface cooling in eastern China. This cooling effect is primarily attributed to increased surface albedo and weakened ET [75–77]. In this context, we conclude that human activities during this period likely contributed to some degree of warming in eastern China, contributing to the contrast in climatic conditions between the mid-Holocene and PI. However, quantifying the exact magnitude and spatial extent of this human-induced warming remains a challenge. Our study underscores the need for more comprehensive paleo-simulations that integrate human activities to fully capture their impact on historical climate patterns.

Dust aerosol emissions are closely associated with the vegetation cover. For example, increased vegetation cover in the Sahara during the mid-Holocene resulted in a reduced dust aerosol loading, with potential effects on the global climate [68,69,78,79]. However, dust aerosol changes are not incorporated in our simulation. Previous studies suggest that the decreased dust emissions in the mid-Holocene contributed to global warming, but it was not the dominant factor for the HTM [16,18]. Nevertheless, its impact should be considered in future studies.

Compared with the results of Thompson et al. [18], our simulations with dynamic vegetation provide more reasonable dynamic

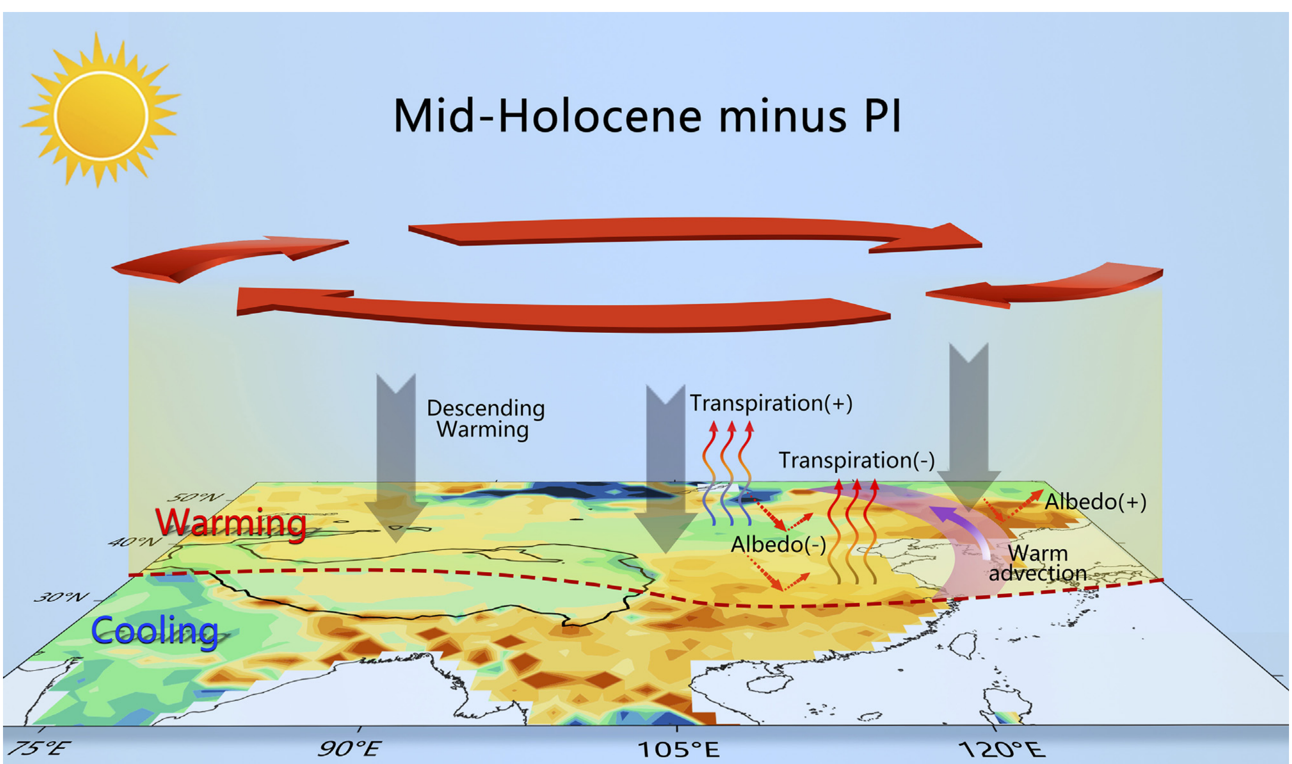

Fig. 5. Schematic diagram of the vegetation-climate feedback on temperature changes in East Asia. The color shading denotes vegetation changes in the mid-Holocene, with green indicating increased vegetation and khaki indicating decreased vegetation. The combined effects of these vegetation changes, including changes in local albedo and ET, along with descending warming and warm advection triggered by anomalies in atmospheric circulation, contributed to the widespread warming observed across most regions of East Asia. This warming effect overcomes the cooling in northern East Asia induced by orbital forcing and changes in GHG concentrations, resulting in a dipolar pattern (south cooling–north warming) of temperature changes in the mid-Holocene compared with the PI.

local vegetation changes and a more detailed picture of the heterogenous pattern of temperature changes in East Asia, such as the cooling on the southern TP (Fig. S13b, d online). This improvement advances our understanding of the Holocene evolution of climate and ecosystems in East Asia, emphasizing the necessity of paleoclimate simulations coupled with a dynamic vegetation module.

To sum up, our study highlights the importance of vegetation-climate feedback in explaining the spatially heterogeneous temperature changes in East Asia during the mid-Holocene. These findings contribute to the growing body of evidence supporting the critical role of vegetation in shaping regional and global climate patterns. Furthermore, they underscore the need to consider both natural and anthropogenic factors in paleoclimate simulations to improve our understanding of past, present, and future climate dynamics. By addressing these limitations and incorporating additional factors such as human activities and dust aerosol emissions, future research can refine our understanding of the complex interplay between vegetation, climate, and human activities and better inform predictions of future climate change.

5. Conclusions

We have employed the fully-coupled Earth system model EC-Earth to investigate the impact of vegetation-climate feedback on temperature anomaly patterns in East Asia during the mid-Holocene. Our simulations included both coupled and decoupled dynamic vegetation, allowing us to isolate the influence of vegetation on regional temperature patterns. The results reveal that vegetation-climate feedback played a significant role in warming most parts of East Asia during the mid-Holocene, resulting in a spatially diverse pattern of temperature changes. Specifically, the northern region experienced warming while the southern region experienced cooling. The inclusion of vegetation-climate feedback greatly improved the agreement between model simulations and reconstructions, highlighting the crucial role of vegetation-climate feedback in resolving the Holocene temperature conundrum.

The simulated vegetation results revealed spatial heterogeneity in the vegetation changes across East Asia during the mid-Holocene. To gain a deeper understanding of the underlying causes of these vegetation changes and their connection to the feedback mechanisms, we utilized the offline dynamic vegetation model LPJ-GUESS and conducted five experiments. The results of these experiments showed that local changes in precipitation and temperature led to divergent vegetation responses in East Asia during the mid-Holocene. Eventually, the combined effects of these vegetation changes, including changes in local albedo and ET, along with atmospheric circulation anomalies resulting from remote vegetation changes, played a major role in the widespread warming observed across most regions of East Asia (Fig. 5). Overall, our study emphasizes the importance of considering vegetation-climate feedback and its complex interactions in understanding past climate variations, particularly during the Holocene period.

Conflict of interest

The authors declare that they have no conflict of interest.

Acknowledgments

This work was supported by the National Natural Science Foundation of China (42101149), the China Postdoctoral Science Foundation (2022M711441), and the Swedish Research Council (Vetenskapsrådet) (2017-04232, 2022-03617). The EC-Earth simulations and the data analysis were performed using ECMWF's computing and archive facilities and the Swedish National Infrastructure for Computing (SNIC) at the National Supercomputer Centre (NSC), partially funded by the Swedish Research Council through grant agreement No. 2018-05913.

Author contributions

Jie Chen contributed the idea for this research and drafted the manuscript. Qiong Zhang designed the EC-Earth simulations and provided supervision, Zhengyao Lu conducted the offline LPJ-GUESS simulations. Yanwu Duan collected the temperature reconstruction data. Xianyong Cao contributed to the collection of biome reconstructions. Jianping Huang and Fahu Chen provided supervision. All authors discussed the results throughout the research and contributed to the writing.

Appendix A. Supplementary materials

Supplementary materials to this article can be found online at https://doi.org/10.1016/j.scib.2024.04.012.

Data availability

The model data used to produce the main figures in this article are accessible at https://doi.org/10.17043/zhang-2023-holocene-vegetation-1. The CMIP6 model data can be downloaded at https://esgf-node.llnl.gov/search/cmip6/.

References

[1] Marcott SA, Shakun JD, Clark PU, et al. A reconstruction of regional and global temperature for the past 11,300 years. Science 2013;339:1198–201.
[2] Zhang W, Wu H, Geng J, et al. Model-data divergence in global seasonal temperature response to astronomical insolation during the Holocene. Sci Bull 2022;67:25–8.
[3] Liu Z, Zhu J, Rosenthal Y, et al. The Holocene temperature conundrum. Proc Natl Acad Sci USA 2014;111:E3501–5.
[4] Kaufman D, McKay N, Routson C, et al. A global database of Holocene paleotemperature records. Sci Data 2020;7:115.
[5] Kaufman D, McKay N, Routson C, et al. Holocene global mean surface temperature, a multi-method reconstruction approach. Sci Data 2020;7:201.
[6] Osman MB, Tierney JE, Zhu J, et al. Globally resolved surface temperatures since the Last Glacial Maximum. Nature 2021;599:239–44.
[7] Hou J, Li C-G, Lee S. The temperature record of the Holocene: Progress and controversies. Sci Bull 2019;64:565–6.
[8] Bova S, Rosenthal Y, Liu Z, et al. Seasonal origin of the thermal maxima at the Holocene and the last interglacial. Nature 2021;589:548–53.
[9] Dong Y, Wu N, Li F, et al. The Holocene temperature conundrum answered by mollusk records from East Asia. Nat Commun 2022;13:5153.
[10] Zhang W, Wu H, Cheng J, et al. Holocene seasonal temperature evolution and spatial variability over the Northern Hemisphere landmass. Nature Commun 2022;13:5334.
[11] Chen F, Duan Y, Hou J. An 88 ka temperature record from a subtropical lake on the southeastern margin of the Tibetan Plateau (third pole): New insights and future perspectives. Sci Bull 2021;66:1056–7.
[12] Park H-S, Kim S-J, Stewart AL, et al. Mid-holocene Northern Hemisphere warming driven by Arctic amplification. Sci Adv 2019;5:eaax8203.
[13] Chen J, Zhang Q, Kjellström E, et al. The contribution of vegetation-climate feedback and resultant sea ice loss to amplified Arctic warming during the mid-Holocene. Geophys Res Lett 2022:e2022GL098816.
[14] Park H-S, Kim S-J, Seo K-H, et al. The impact of Arctic Sea ice loss on mid-Holocene climate. Nat Commun 2018;9:4571.
[15] Zhang X, Chen F. Non-trivial role of internal climate feedback on interglacial temperature evolution. Nature 2021;600:E1–3.
[16] Liu Y, Zhang M, Liu Z, et al. A possible role of dust in resolving the Holocene temperature conundrum. Sci Rep 2018;8:4433.
[17] Foley JA, Kutzbach JE, Coe MT, et al. Feedbacks between climate and boreal forests during the Holocene epoch. Nature 1994;371:52–4.
[18] Thompson AJ, Zhu J, Poulsen CJ, et al. Northern Hemisphere vegetation change drives a Holocene thermal maximum. Sci Adv 2022;8:eabj6535.
[19] Timmermann A, Sachs J, Timm OE. Assessing divergent SST behavior during the last 21 ka derived from alkenones and G. ruber-Mg/Ca in the equatorial Pacific. Paleoceanogr Paleoclimatol 2014;29:680–96.
[20] Marsicek J, Shuman BN, Bartlein PJ, et al. Reconciling divergent trends and millennial variations in Holocene temperatures. Nature 2018;554:92–6.

[21] Bader J, Jungclaus J, Krivova N, et al. Global temperature modes shed light on the Holocene temperature conundrum. Nat Commun 2020;11:4726.
[22] Cartapanis O, Jonkers L, Moffa-Sanchez P, et al. Complex spatio-temporal structure of the Holocene thermal maximum. Nat Commun 2022;13:5662.
[23] Chen F, Duan Y, Hao S, et al. Holocene thermal maximum mode versus the continuous warming mode: Problems of data-model comparisons and future research prospects. Sci China Earth Sci 2023;66:1683–701.
[24] Kaufman DS, Broadman E. Revisiting the Holocene global temperature conundrum. Nature 2023;614:425–35.
[25] Jiang D, Lang X, Tian Z, et al. Considerable model–data mismatch in temperature over China during the mid-Holocene: Results of PMIP simulations. J Clim 2012;25:4135–53.
[26] Tian F, Cao X, Dallmeyer A, et al. Quantitative woody cover reconstructions from eastern continental Asia of the last 22 kyr reveal strong regional peculiarities. Quat Sci Rev 2016;137:33–44.
[27] Lu Z, Miller PA, Zhang Q, et al. Dynamic vegetation simulations of the mid-Holocene Green Sahara. Geophys Res Lett 2018;45:8294–303.
[28] Lindgren A, Lu Z, Zhang Q, et al. Reconstructing past global vegetation with random forest machine learning, sacrificing the dynamic response for robust results. J Adv Modeling Earth Syst 2021;13:e2020MS002200.
[29] Kukla T, Ahlström A, Maezumi SY, et al. The resilience of Amazon tree cover to past and present drying. Global Planet Change 2021;202:103520.
[30] Döscher R, Acosta M, Alessandri A, et al. The EC-Earth3 earth system model for the coupled model intercomparison project 6. Geosci Model Dev 2022;15:2973–3020.
[31] Balsamo G, Beljaars A, Scipal K, et al. A revised hydrology for the ECMWF model: Verification from field site to terrestrial water storage and impact in the integrated forecast system. J Hydrometeorol 2009;10:623–43.
[32] Madec G. Nemo Ocean engine: Note du pole de modélisation. Institut Pierre-Simon Laplace (IPSL) 2008;27:1288–619.
[33] Rousset C, Vancoppenolle M, Madec G, et al. The Louvain-la-Neuve Sea ice model LIM3.6: Global and regional capabilities. Geosci Model Dev 2015;8:2991–3005.
[34] Smith B, Wårlind D, Arneth A, et al. Implications of incorporating N cycling and N limitations on primary production in an individual-based dynamic vegetation model. Biogeosciences 2014;11:2027–54.
[35] Harrison S. BIOME 6000 DB classified plotfile version 1. 2017.
[36] Prentice I, Harrison S, Bartlein P. Global vegetation and terrestrial carbon cycle changes after the last ice age. New Phytol 2011;189:988–98.
[37] An C-B, Chen F-H, Barton L. Holocene environmental changes in Mongolia: A review. Global Planet Change 2008;63:283–9.
[38] Klinge M, Sauer D. Spatial pattern of Late Glacial and Holocene climatic and environmental development in Western Mongolia - A critical review and synthesis. Quat Sci Rev 2019;210:26–50.
[39] Li N, Song L, Sack D, et al. Phytolith and simulation evidence for precipitation-modulated vegetation dynamics along the East Asian monsoon margin. Palaeogeogr Palaeoclimatol Palaeoecol 2022;590:110842.
[40] Stebich M, Rehfeld K, Schluetz F, et al. Holocene vegetation and climate dynamics of NE China based on the pollen record from Sihailongwan Maar Lake. Quat Sci Rev 2015;124:275–89.
[41] Gong Z, Chen H, Yuan D, et al. The temporal and spatial distribution of ancient rice in China and its implications. Chin Sci Bull 2007;52:1071–9.
[42] Meng Y, Wang W, Hu J, et al. Vegetation and climate changes over the last 30 000 years on the Leizhou peninsula, southern China, inferred from the pollen record of Huguangyan Maar Lake. Boreas 2017;46:525–40.
[43] Wang W, Li C, Shu J, et al. Changes of vegetation in southern China. Sci China Earth Sci 2019;62:1316–28.
[44] Cao X, Tian F, Herzschuh U, et al. Human activities have reduced plant diversity in eastern China over the last two millennia. Glob Change Biol 2022;28:4962–76.
[45] Shi J, Li D, Xu Q, et al. Land cover reconstruction in Northwest China since 6 ka BP: Preliminary application of a new strategy. Qua Int 2022;641:25–38.
[46] Li F, Gaillard M-J, Cao X, et al. Towards quantification of Holocene anthropogenic land-cover change in temperate China: A review in the light of pollen-based REVEALS reconstructions of regional plant cover. Earth-Sci Rev 2020;203:103119.
[47] Zhang Y, Marquer L, Cui Q, et al. Holocene vegetation changes in the transition zone between subtropical and temperate ecosystems in eastern Central China. Quat Sci Rev 2021;253:106768.
[48] Chen J, Zhang Q, Huang W, et al. Northwestward shift of the northern boundary of the East Asian summer monsoon during the mid-Holocene caused by orbital forcing and vegetation feedbacks. Quat Sci Rev 2021;268:107136.
[49] Chen F, Xu Q, Chen J, et al. East Asian summer monsoon precipitation variability since the last deglaciation. Sci Rep 2015;5:11186.
[50] Xu Q, Chen F, Zhang S, et al. Vegetation succession and East Asian summer monsoon changes since the last deglaciation inferred from high-resolution pollen record in Gonghai Lake, Shanxi province. China. Holocene 2017;27:835–46.
[51] Cao X, Herzschuh U, Ni J, et al. Spatial and temporal distributions of major tree taxa in eastern continental Asia during the last 22,000 years. Holocene 2015;25:79–91.
[52] Liu Y, Song H, Sun C, et al. The 600-mm precipitation isoline distinguishes tree-ring-width responses to climate in China. Natl Sci Rev 2019;6:359–68.
[53] Cai Q, Liu Y, Wang Y, et al. Recent warming evidence inferred from a tree-ring-based winter-half year minimum temperature reconstruction in northwestern Yichang, South Central China, and its relation to the large-scale circulation anomalies. Int J Biometeorol 2016;60:1885–96.
[54] Yu J, Zhou G, Liu Q. Tree-ring based summer temperature regime reconstruction in XiaoXing Anling Mountains, northeastern China since 1772 CE. Palaeogeogr Palaeoclimatol Palaeoecol 2018;495:13–23.
[55] Jiang Y, Yuan X, Zhang J, et al. Reconstruction of June–July temperatures based on a 233 year tree-ring of *Picea jezoensis* var. *microsperma*. Forests 2019;10:416.
[56] Zhang W, Shi J, Zhao Y, et al. December–March temperature reconstruction from tree-ring earlywood width in southeastern China during the period of 1871–2016. Int J Biometeorol 2021;65:883–94.
[57] van den Hurk BJ, Viterbo P, Los SO. Impact of leaf area index seasonality on the annual land surface evaporation in a global circulation model. J Geophys Res-Atmos 2003;108:4191.
[58] Notaro M, Chen G, Liu Z. Vegetation feedbacks to climate in the global monsoon regions. J Clim 2011;24:5740–56.
[59] Lee S, Lee MI. Effects of surface vegetation on the intensity of East Asian summer monsoon as revealed by observation and model experiments. Int J Climtol 2020;40:3634–48.
[60] Li Q, Ma M, Wu X, et al. Snow cover and vegetation-induced decrease in global albedo from 2002 to 2016. J Geophys Res-Atmos 2018;123:124–38.
[61] Yan H, Wang S, Dai J, et al. Forest greening increases land surface albedo during the main growing period between 2002 and 2019 in China. J Geophys Res-Atmos 2021;126:e2020JD033582.
[62] Li X, Qu Y, Xiao Z. Reponses of land surface albedo to global vegetation greening: An analysis using GLASS data. Atmos 2023;14:31.
[63] Peng S-S, Piao S, Zeng Z, et al. Afforestation in China cools local land surface temperature. Proc Natl Acad Sci USA 2014;111:2915–9.
[64] Shen M, Piao S, Jeong S-J, et al. Evaporative cooling over the Tibetan Plateau induced by vegetation growth. Proc Natl Acad Sci USA 2015;112:9299–304.
[65] Liu Z, Notaro M, Kutzbach J, et al. Assessing global vegetation–climate feedbacks from observations. J Clim 2006;19:787–814.
[66] Binder H, Boettcher M, Grams CM, et al. Exceptional air mass transport and dynamical drivers of an extreme wintertime Arctic warm event. Geophys Res Lett 2017;44:12,028-12,036.
[67] Wang P, Tang J, Sun X, et al. Heat waves in China: Definitions, leading patterns, and connections to large-scale atmospheric circulation and SSTs. J Geophys Res-Atmos 2017;122:10,679-10,699.
[68] Sun W, Wang B, Zhang Q, et al. Northern Hemisphere land monsoon precipitation increased by the Green Sahara during middle Holocene. Geophys Res Lett 2019;46:9870–9.
[69] Sun W, Wang B, Zhang Q, et al. Middle East climate response to the Saharan vegetation collapse during the mid-Holocene. J Clim 2021;34:229–42.
[70] Zhang C, Zhao C, Yu S-Y, et al. Seasonal imprint of Holocene temperature reconstruction on the Tibetan Plateau. Earth-Sci Rev 2022;226:103927.
[71] Feng X, Zhao C, D'Andrea WJ, et al. Evidence for a relatively warm mid- to late Holocene on the southeastern Tibetan Plateau. Geophys Res Lett 2022;49:e2022GL098740.
[72] Zhao C, Rohling EJ, Liu Z, et al. Possible obliquity-forced warmth in southern Asia during the Last Glacial Stage. Sci Bull 2021;66:1136–45.
[73] Rao Z, Shi F, Li Y, et al. Long-term winter/summer warming trends during the Holocene revealed by α-cellulose $\delta^{18}O/\delta^{13}C$ records from an alpine peat core from central Asia. Quat Sci Rev 2020;232:106217.
[74] Huang X, Ren X, Chen X, et al. Anthropogenic mountain forest degradation and soil erosion recorded in the sediments of Mayinghai Lake in northern China. Catena 2021;207:105597.
[75] Pongratz J, Reick C, Raddatz T, et al. Biogeophysical versus biogeochemical climate response to historical anthropogenic land cover change. Geophys Res Lett 2010;37:L08702.
[76] He F, Vavrus SJ, Kutzbach JE, et al. Simulating global and local surface temperature changes due to Holocene anthropogenic land cover change. Geophys Res Lett 2014;41:623–31.
[77] Smith MC, Singarayer JS, Valdes PJ, et al. The biogeophysical climatic impacts of anthropogenic land use change during the Holocene. Clim Past 2016;12:923–41.
[78] Pausata FS, Emanuel KA, Chiacchio M, et al. Tropical cyclone activity enhanced by Sahara greening and reduced dust emissions during the African Humid Period. Proc Natl Acad Sci USA 2017;114:6221–6.
[79] Pausata FS, Zhang Q, Muschitiello F, et al. Greening of the Sahara suppressed ENSO activity during the mid-Holocene. Nat Commun 2017;8:16020.

Jie Chen is young researcher at Key Laboratory of Western China's Environmental Systems, College of Earth and Environmental Sciences, Lanzhou University. She earned her doctorate from Lanzhou University in 2021. Her recent research focuses on paleo-vegetation changes and their climate impact by using climate model.

Qiong Zhang is a professor in paleoclimate modelling at the Department of Physical Geography at Stockholm University. She and her team use the Earth system model EC-Earth to understand climate change and climate variability from past to future.